

# Vascular Dysmorphogenesis Caused by an Activating Mutation in the Receptor Tyrosine Kinase TIE2

Miikka Vikkula,<sup>1,7</sup> Laurence M. Boon,<sup>1,2,7,8</sup>  
Kermit L. Carraway III,<sup>3</sup> Jennifer T. Calvert,<sup>4</sup>  
A. John Diamonti,<sup>3</sup> Boyan Goumnerov,<sup>5</sup>  
Krystyna A. Pasyk,<sup>6</sup> Douglas A. Marchuk,<sup>4</sup>  
Matthew L. Warman,<sup>1,9</sup> Lewis C. Cantley,<sup>3</sup>  
John B. Mulliken,<sup>2</sup> and Bjorn R. Olsen<sup>1</sup>

<sup>1</sup> Department of Cell Biology  
Harvard Medical School  
Harvard-Forsyth Department of Oral Biology  
Harvard School of Dental Medicine  
Boston, Massachusetts 02115

<sup>2</sup> Division of Plastic Surgery  
Children's Hospital  
Harvard Medical School  
Boston, Massachusetts 02115

<sup>3</sup> Department of Cell Biology  
Harvard Medical School  
Division of Signal Transduction  
Beth Israel-Deaconess Hospital  
Boston, Massachusetts 02115

<sup>4</sup> Department of Genetics  
Duke University Medical Center  
Durham, North Carolina 27710

<sup>5</sup> Department of Pathology  
Children's Hospital  
Harvard Medical School  
Boston, Massachusetts 02115

<sup>6</sup> Institute of Gerontology  
University of Michigan  
Ann Arbor, Michigan 48109

## Summary

Venous malformations (VMs), the most common errors of vascular morphogenesis in humans, are composed of dilated, serpiginous channels. The walls of the channels have a variable thickness of smooth muscle; some mural regions lack smooth muscle altogether. A missense mutation resulting in an arginine-to-tryptophan substitution at position 849 in the kinase domain of the receptor tyrosine kinase TIE2 segregates with dominantly inherited VM in two unrelated families. Using proteins expressed in insect cells, we demonstrate that the mutation results in increased activity of TIE2. We conclude that an activating mutation in TIE2 causes inherited VMs in the two families and that the TIE2 signaling pathway is critical for endothelial cell-smooth muscle cell communication in venous morphogenesis.

## Introduction

Vascular morphogenesis begins as vasculogenesis, in situ differentiation of endothelial cells (ECs) from hemangioblasts, and subsequent formation of endothelial

tubes (Risau and Lemmon, 1988; Risau et al., 1988; Noden, 1989). This retiform plexus undergoes remodeling and forms the complex network of adult vasculature through angiogenesis, the sprouting of new blood vessels from preexisting ones (Risau et al., 1988; Noden, 1989).

Formation of endothelial tubes is followed by recruitment of pericytes and smooth muscle cells (SMCs) from mesenchymal progenitor cells and neural crest cells (Nakamura, 1988; Kirby and Waldo, 1995). ECs are believed to play an important role in regulating this recruitment. For example, in EC-SMC cocultures, ECs stimulate proliferation (Fillinger et al., 1993) and induce migration of SMCs (Powell et al., 1996a). Furthermore, in organ cultures of human saphenous veins, denudation of the endothelium results in decreased proliferation of intimal SMCs (Allen et al., 1994). ECs can also modulate the morphology of SMCs from a synthetic to a contractile phenotype (Powell et al., 1996b).

Several cytokines and growth factors have been implicated in these effects. Platelet-derived growth factor (PDGF) expressed by ECs acts as a mitogen and chemoattractant for mesenchymal cells in vitro (Grotendorst et al., 1981; Grotendorst et al., 1982; Westermark et al., 1990). Another growth factor, transforming growth factor  $\beta_1$  (TGF $\beta_1$ ), also known to be produced by ECs, induces differentiation of neural crest cells into SMCs (Shah et al., 1996). Signaling from the mesenchymal cells and extracellular matrix to endothelium is also likely, since a single cell population, the hemangioblasts, gives rise to ECs in arterial, capillary, venous, and lymphatic vessels, which are known to differ in their pattern of gene expression. For example, lymphatic ECs have high expression of VEGFR-3/FLT-4, whereas the expression of this cytokine receptor in veins and arteries is almost undetectable (Kaipainen et al., 1995). Furthermore, extracellular matrix can modulate the effects of ECs on SMC migration and adhesiveness (Powell et al., 1996a), and EC proliferation can be inhibited by contact with SMCs and pericytes (Orlidge and D'Amore, 1987). As a result, there are structural differences in the walls of mature vessels in different segments of the vascular tree, and cell signaling pathways are likely to differ in morphologically or functionally distinctive segments of the vascular system.

Genetic vascular disorders in humans provide molecular insights into these pathways. For example, hereditary hemorrhagic telangiectasia (Rendu-Osler-Weber syndrome), in which there is a gradual alteration in the capillary bed between venules and arterioles, has been shown to be caused by mutations in two TGF $\beta$  binding proteins, endoglin and activin receptor-like kinase (McAllister et al., 1994; Johnson et al., 1996). As a result of localized capillary dilatation, arterial blood is shunted directly into postcapillary venules, which in turn become

<sup>7</sup> These authors contributed equally to this work.

<sup>8</sup> Current address: Division of Plastic Surgery, Catholic University

of Louvain, 10 Avenue Hippocrate, 1200 Brussels, Belgium.

<sup>9</sup> Present address: Department of Genetics, Case Western Reserve University School of Medicine, Cleveland, Ohio 44106.

convoluted and "arterialized," manifesting increased smooth muscle within their walls. These findings suggest that TGF $\beta$  signaling pathways are crucial for the development and maintenance of normal capillary beds. In ataxia-telangiectasia, intracellular signaling errors due to mutations in a protein kinase/phosphatidylinositol kinase homolog cause abnormalities in cell cycle control, resulting in telangiectases (Savitsky et al., 1995).

Venous malformation (VM) is the most common developmental vascular anomaly. VMs are usually sporadic and solitary, but they can also be familial and typically are multifocal. They are usually located in skin and mucosal membranes, but any organ can be affected (Mulliken and Young, 1988). VMs are seen either at birth or later in life. The molecular basis for VMs is unknown. To gain insight into the cause of VM, we have studied two unrelated families with dominantly inherited mucocutaneous VMs. Using random linkage mapping, we found that the locus for a gene causing the malformations is on the short arm of chromosome 9 (Boon et al., 1994; Gallione et al., 1995). Here we report that the receptor tyrosine kinase TIE2 gene is localized within this locus, and that a C-to-T nucleotide transition, leading to an arginine-to-tryptophan substitution at position 849 (R849W) in the kinase domain of the receptor, cosegregates with the phenotype in the two families. Furthermore, by using a baculovirus expression system, we demonstrate that the R849W change causes increased activity of the TIE2 kinase. Using immunohistochemistry of lesions, we also show that affected vessels contain a disproportionately large number of ECs versus SMCs. Therefore, we conclude that the developmental venous anomalies in the two families are caused by local uncoupling between the normal recruitment of SMCs and the proliferation of ECs. This uncoupling is due to an activating mutation in TIE2 and indicates that the TIE2 signaling pathway is crucial for the normal development of veins.

## Results

### Inherited VM in Two Families Is Linked to an Interval on Chromosome 9p21

We have described linkage of inherited VM in two families to markers on the short arm of chromosome 9 (VMCM1; OMIM number 600195) (Boon et al., 1994; Gallione et al., 1995). The linked interval was defined by recombinant markers *D9S157* and *D9S161*. We evaluated 35 additional members of the family SA (Figure 1A) and narrowed the interval to 8 centimorgans (cM) between the *IFN* gene cluster and marker *D9S161* (data not shown). Three members of family SA and one member of family AF were recombinant for the entire interval. Individual II-15 in family SA had a single cervical lesion but had not inherited the haplotype linked to the disease, whereas unaffected individuals IV-9, a 14-year-old boy, and II-21, an 81-year-old man, had inherited the haplotype. The cervical lesion in individual II-15 appeared in early adulthood, whereas lesions in her relatives were multiple and became apparent clinically at an earlier age. It is therefore probable that she represents a sporadic case. Individual IV-16, an unaffected 32-year-old woman in family AF, also had inherited the haplotype linked to the disease (Figure 1B). We assume that the

three unaffected individuals IV-9, II-21, and IV-16 are nonpenetrant for the disease phenotype.

### The Receptor Tyrosine Kinase TIE2 Gene Is Localized within the VMCM1 Locus

For positional cloning and candidate gene identification, we obtained two human melanoma cell lines (MN455 and W) containing previously defined homozygous deletions of 9p and a YAC contig covering the 8 cM region from the *IFN* gene cluster to the marker *D9S161* (generously provided by Dr. Frank Haluska). The EC-specific receptor tyrosine kinase TIE2 gene had been mapped previously to 9p21 by in situ hybridization (Dumont et al., 1994); we wanted to test whether it was localized to the linked interval. Using DNA from the cell lines and YAC clones as template for polymerase chain reaction (PCR), we found that DNA from cell line MN455 was positive for TIE2, whereas DNA from cell line W was negative. Since cell line MN455 has a deletion of the *IFN* gene cluster and cell line W is deleted between *IFNA* and *D9S3*, the TIE2 gene had to lie between these markers. Of the 24 tested YAC clones, IG4D7, 711C4, 874c7, 822f8, 899b9, and 882f4 were positive with TIE2-specific PCR. Since these clones were also positive for *D9S169* (located between *IFNA* and *D9S3*), and the smallest of the clones, 874c7, was 560 kb in size, the TIE2 gene had to lie in the vicinity of this marker within the linked interval.

### A Single Nucleotide Change in TIE2 Segregates with the Phenotype in Two Unrelated VM families

To analyze TIE2 as a candidate gene in the two VM families, we used Epstein-Barr virus to transform lymphocytes taken from two patients in family SA (individuals III-7 and II-13, Figure 1), one patient in family AF (individual IV-13, Figure 1B), and control individuals. We extracted total RNA from the cultured cells and used it as template for reverse transcription PCR. PCR primers for nine overlapping fragments were synthesized to cover the whole 3375 bp coding sequence of the TIE2 gene. Cycle sequencing of these products identified: two nucleotide polymorphisms that do not change the codon for an amino acid (G1962A and G2322A); a single-amino acid-deletion polymorphism (valine 788; bovine and rat sequences have the valine residue and the murine does not); and a T2084C change resulting in an isoleucine-to-threonine substitution that was confirmed to be homozygous in our samples and in a partial human TIE2 clone (kindly provided by Dr. Kari Alitalo). In the murine, bovine, and rat sequences, a threonine residue is found at this position, suggesting that threonine 2084 is an error in the previously published human sequence.

We also identified a C-to-T transition at position 2545 that changes an arginine to a tryptophan residue (Figure 2A). To confirm that the C2545T transition was present in genomic DNA and that this nucleotide substitution cosegregated with the phenotype in family SA, we tested all 61 family members with allele-specific PCR (Figure 2B). All affected individuals carried this change, except II-15, who was recombinant for the whole region. In addition, the unaffected individuals IV-9 and II-21 carried this nucleotide substitution. We also tested 138 control

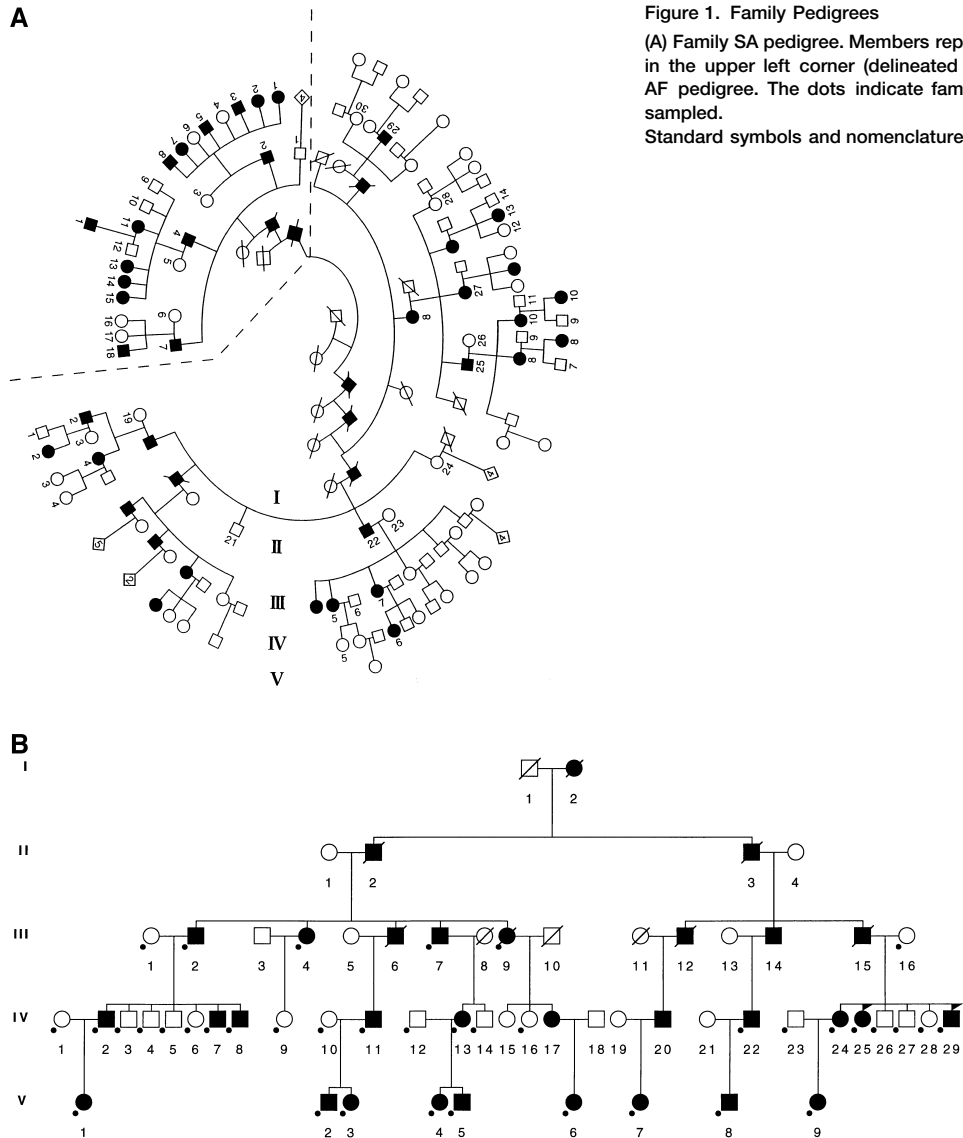


Figure 1. Family Pedigrees

(A) Family SA pedigree. Members reported previously are clustered in the upper left corner (delineated by a dotted line). (B) Family AF pedigree. The dots indicate family members who have been sampled. Standard symbols and nomenclature are used.

individuals from Canada, Finland, and the United States, but none of them had the C-to-T transition.

To test whether the same nucleotide change, C2545T, existed in family AF, genomic DNA from all family members was amplified and evaluated with a MaeIII restriction fragment-length analysis, since the mutation destroys a MaeIII site. All affected individuals as well as the unaffected individual IV-16 were heterozygous for the substitution. To rule out that this nucleotide change was a founder mutation and that the two families may be related, we genotyped affected individuals from both families for the sizes of associated STRP alleles. The linked haplotypes differed from each other both for flanking markers as well as for an intragenic nucleotide polymorphism (Figure 3).

**The R849W Mutation in TIE2 Causes Kinase Activation**

The mutated arginine 849, located six amino acid residues upstream of the invariant lysine in the first intracellular kinase domain of TIE2 (see below), is conserved in

the human, bovine, murine, and rat sequences (GenBank accession numbers L06139, X71424, X71426, and 386048). In the homologous TIE1 receptor, the arginine is replaced by a lysine in the human, bovine, and murine sequences (GenBank accession numbers X60957, X71423, and X71425). This suggests that a basic residue in this position is important for the kinase structure or function.

To study the biochemical effect of this change on kinase function, we cloned the full-length wild-type and mutant TIE2 cDNA into a baculovirus expression vector. Recombinant viruses were obtained and several clones were purified. Using rabbit anti-TIE2 antibody (Santa Cruz), TIE2 protein was immunoprecipitated from insect cell extracts. Western blotting showed a specific 140 kDa band, the expected size for TIE2 (Figure 4A); immunoblotting with anti-phosphotyrosine antibodies showed that both wild-type and mutant receptors in the extracts were autophosphorylated, but the mutated receptor protein was phosphorylated to a higher extent than the wild-type protein (data not shown). In addition,

when the immunoprecipitates were incubated with [ $\gamma$ - $^{32}$ P]ATP before gel electrophoresis, autoradiography suggested that the mutant receptor had a 6- to 10-fold higher autophosphorylation activity in vitro than the wild-type receptor (Figure 4A).

The wild-type and mutant receptors were also incubated with a synthetic tyrosine-oriented peptide library (Songyang et al., 1995) to assay for differences in the ability to phosphorylate peptide substrates. The phosphorylated peptides were separated from nonphosphorylated peptides and sequenced. We detected no differences in specificity between the wild-type and mutant receptors. However, the mutant protein was much more active at phosphorylating peptides in the library (Figure 4B).

### VMs Contain a Disproportionately High Ratio of ECs to SMCs

VMs excised from members of family SA showed dilated vascular channels of variable diameter (Figures 5A and 5B). Specimen II-7 exhibited only few ectatic veins, whereas specimen II-8, taken from a large anomaly affecting one third of the tongue (for clinical picture, see Boon et al., 1994), and specimen II-5 (Figure 5) were composed of numerous serpiginous channels. Of note,

veins and arteries with normal structure were seen adjacent to abnormal channels within the tissue specimens (Figure 5C).

Immunostaining with antibodies against CD31 (data not shown) and von Willebrand factor (vWF) showed specific staining of the luminal cells lining blood vessel walls (Figure 5A). Positive vWF staining was also seen in intraluminal platelets. With high magnification, flattened ECs were seen to line the abnormal channels. Endothelial nuclei were located far apart from one another, but there was no endothelial discontinuity.

Antibodies against SMC  $\alpha$ -actin demonstrated specific but patchy and irregular staining of the abnormal channels as compared with the uniform layer of stained cells around normal veins (Figures 5B and 5C). In the abnormal channels the staining intensity varied with the size of the vessels. Small channels typically showed prominent staining, as compared to larger channels, some of which were devoid of  $\alpha$ -actin staining. Scattered SMCs were discernible at high magnification. Disorganized smooth muscle was seen in the adjacent vessel wall whenever there was evidence of a mural thrombus, a pathognomonic finding in VMs.

### Discussion

#### VM Is Caused by a Mutation in the TIE2 Receptor Tyrosine Kinase

Based on the localization of the TIE2 gene in the minimal candidate interval of 8 cM, the identification of the same nucleotide transition in affected individuals of two unrelated families, and the increased kinase activity of the mutant receptor in vitro, we conclude that VMs are caused by a mutation in the TIE2 receptor. This is supported by the EC-specific expression pattern of TIE2 (Dumont et al., 1995).

We have shown that a nucleotide transition, C2545T, results in an R849W substitution. This is not a common polymorphism because the C-to-T transition was not detected in 138 control individuals. The same mutation was also identified in two disparate VM families. Family SA is of Italian origin and family AF of German origin, and thus it is unlikely that the mutated allele could be derived from a common ancestor. Indeed, haplotype analyses of flanking markers and an intragenic polymorphism demonstrated that the mutations occurred in two

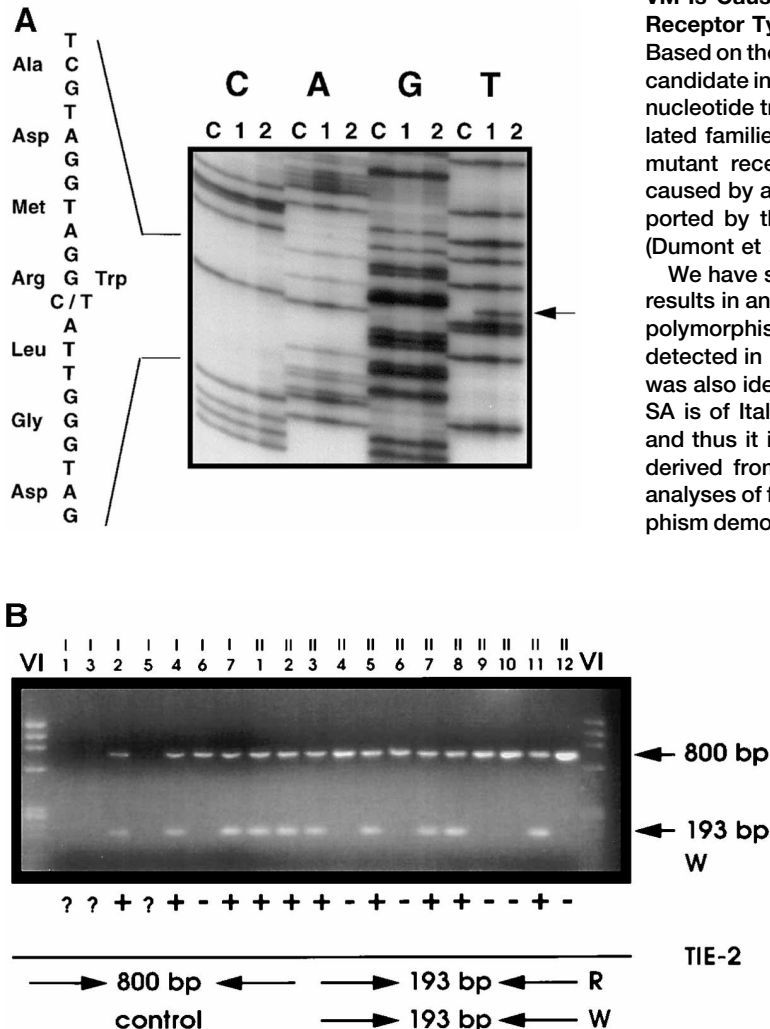


Figure 2. Detection of the Missense Mutation in TIE2 in Family SA

(A) Sequencing gel showing the C-to-T change (arrow) in two affected individuals of family SA (lanes 2 and 3). C, control. (B) Allele-specific PCR of 19 individuals of family SA (see Figure 1A) showing amplification of the mutant allele (193 bp) with an internal control (800 bp). VI, size marker; plus, carrier; minus, normal; question mark, sample did not work.

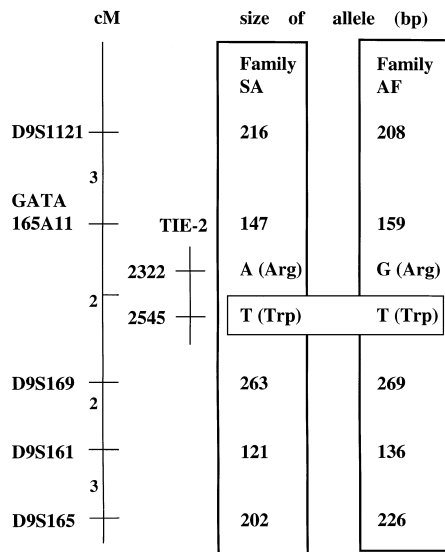


Figure 3. Haplotypes of Linked Alleles for One TIE2 Intragenic Polymorphism (G2322A) and Five Flanking Markers in the Two Unrelated VM Families

The C2545T mutation is flanked by different alleles of the intragenic G2322A polymorphism and either *D9S169* or *GATA165A11* in the two families, since the orientation of the TIE2 gene on the chromosome is unknown. TIE2 and *D9S169* are maximally 560 kb apart, the size of the smallest YAC clone, y874c7, containing both markers.

different TIE2 alleles, suggesting that the R849W change could be localized in a mutational "hot spot." The mutations occurred in a CpG dinucleotide, often associated with transitional mutations. An example of a similar "hot spot" is achondroplasia, in which up to 97% of the mostly sporadic, de novo mutations result in substitution of a single amino acid residue (G380R) in the transmembrane domain of fibroblast growth factor receptor 3 (FGFR3) (Bellus et al., 1995).

Of note, a single-amino acid-length polymorphism was also identified in the kinase domain of the TIE2 receptor. The polymorphic valine residue (788) is not present in the murine TIE2 sequence but is present in the bovine and rat TIE2. The length variations between the murine, human, and bovine sequences (1122, 1124, and 1125 amino acid residues, respectively) suggest that small differences in the number of amino acids can occur without interruption of the function of the protein. We confirmed that it is a polymorphism by identifying homozygous and heterozygous individuals for the absence of valine 788.

#### The R849W Mutation Causes Increased Phosphorylation Activity of TIE2

Overexpression studies of full-length wild-type and mutant receptors in insect cells showed an increase in autophosphorylation activity for the mutant form. Not only was the mutant protein more phosphorylated than the wild-type protein when assayed directly by immunoblotting of insect cell extracts, it also showed a 6- to 10-fold higher autophosphorylation activity *in vitro* when incubated with [ $\gamma$ - $^{32}$ P]ATP. Like many other growth factor receptors, TIE2 is easily autophosphorylated when

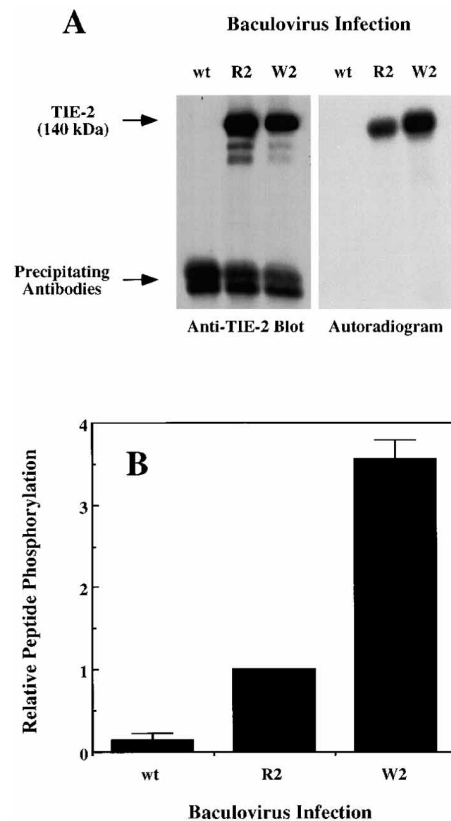


Figure 4. Comparison of the Kinase Activities of Normal and Mutant TIE2 Receptors

(A) Lysates from Sf9 insect cells infected with wild-type baculovirus (wt) or virus expressing normal TIE2 (R2) or mutant TIE2 (W2) were immunoprecipitated with anti-TIE2 antibody and incubated with radiolabeled ATP. Precipitates were subjected to autoradiography (right) and blotted with anti-TIE2 (left).

(B) Anti-TIE2 immunoprecipitates described in (A) were used to phosphorylate an oriented random peptide library. Shown is the observed peptide phosphorylation for each of the precipitates, normalized to the activity associated with the wild-type TIE2 receptor. Since the expression levels of R2 are 2- to 3-fold higher than those of W2, the autophosphorylation and substrate phosphorylation activities of mutant TIE2 are 6- to 10-fold those of wild-type receptor. Error bars, standard error of three independent experiments.

overexpressed, even without ligand. It has been suggested that receptors that need ligand binding for dimerization and subsequent autophosphorylation have a weaker intrinsic inhibitory mechanism of autophosphorylation (Mohammadi et al., 1996). This may be true for TIE2, which is believed to form dimers after ligand binding.

How does the R849W change increase kinase activity? The substituted arginine 849 is located six residues upstream of the invariant lysine in the kinase domain and is conserved among human, bovine, murine, and rat TIE2 sequences; in the homologous receptor, TIE1, another basic amino acid residue, lysine, is found at the same position in the human, bovine, and murine sequences. This suggests that a basic residue is important at this position. In the crystal structure of the FGFR1 kinase domain, an arginine residue, 38 amino acid residues upstream of the invariant lysine, is found hydrogen-bonded to the carbonyl group of a downstream proline

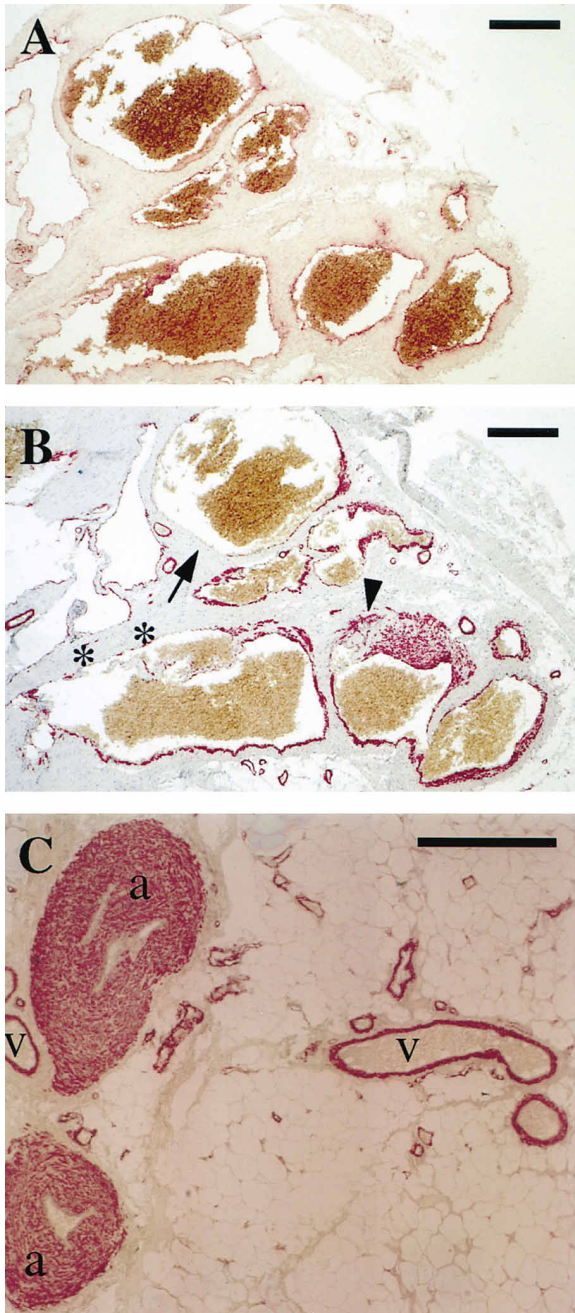


Figure 5. Immunohistochemistry of VM Lesion with Antibodies against vWF (A) and SMC  $\alpha$ -Actin (B and C)  
(A) Staining with vWF antibodies shows a continuous covering of ECs in the large veins. (B) In contrast, staining with antibodies against  $\alpha$ -actin shows that the malformed veins contain regions of disorganized SMCs (arrowhead), regions with no detectable staining (arrow), and regions with a thin, uneven layer of smooth muscle (asterisks). (C) Normal veins (v) and arteries (a) are found adjacent to the malformed veins within the specimen. Scale bars, 200  $\mu$ M.

residue, suggesting an important role in the stabilization of the amino-terminal lobe of the kinase domain (Mohammadi et al., 1996). If arginine 849 in TIE2 is involved similarly in stabilizing the kinase domain, it could be that its substitution by tryptophan alters the conformation

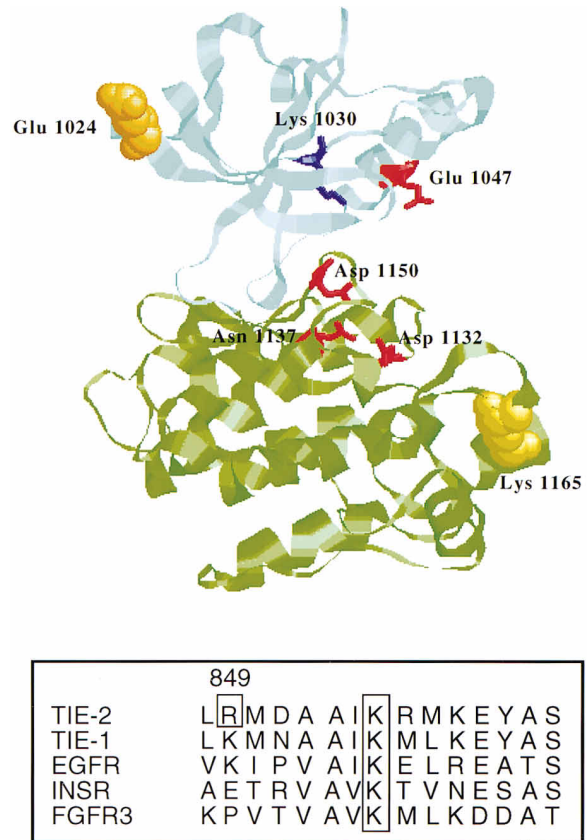


Figure 6. Kinase Domain Structure and Partial Amino Acid Sequence

(Top) Ribbon structure of the insulin receptor kinase domain, illustrating the location of the activating mutation in the TIE2 receptor kinase. The amino-terminal lobe is depicted in blue and the carboxy-terminal lobe is depicted in green. The side chains of amino acid residues involved in catalysis (Glu 1047, Asp 1132, Asn 1137, and Asp 1150) are depicted in red. The conserved lysine residue necessary for activity (Lys 1030) is shown in purple. A glutamic acid residue (Glu 1024) corresponding to the residue mutated in TIE2 is depicted by orange space-filling atoms, emphasizing that this residue is at a position distal to the catalytic cleft. A lysine residue (Lys 1126) corresponding to the K650E mutation in the activation loop of FGFR3 is illustrated with yellow space-filling atoms.

(Bottom) Amino acid sequences in the region of the R849W mutation are shown for five human tyrosine kinase receptors, including the insulin receptor. The invariant lysine (K) residue and the arginine (R) 849 in TIE2 are indicated by boxes.

of this domain so that intrinsic inhibitory mechanisms are diminished, resulting in increased autophosphorylation. Alternatively, replacement with a more hydrophobic residue (tryptophan) could induce receptor dimerization in the absence of ligand and result in increased autophosphorylation. It is noteworthy that when the TIE2 sequence is superimposed on the crystal structure of other kinase domains, arginine 849 is located on an outward curving loop (Figure 6), a loop that could be involved in dimerization.

A graded activation of receptor function is seen with certain amino acid substitutions in FGFR3 that cause osteochondrodysplasias of differing severity (Naski et al., 1996; Webster et al., 1996). One of these mutations,

G380R, the cause of achondroplasia, is located in the transmembrane domain and has a weak activating effect on the receptor, resulting in 15%–20% ligand-independent mitogenic activity. Another mutation, K650E, located in the activation loop of the FGFR3 kinase domain (Figure 6), results in a 100-fold increase in autophosphorylation (Webster et al., 1996). Of note, when a number of other residues in the region of lysine 650 (the  $\beta 10$ – $\beta 11$  region) were mutated to glutamine, no activation of the kinase was observed (Webster et al., 1996). Thus, mutations involving residues only at specific locations in FGFR3 alter kinase activity. The R849W mutation in TIE2 may represent a similar case.

Based on the observations of FGFR3 mutations, it has been postulated that they differentially affect dimerization of the receptor and that increasing the amount of mutated protein would result in increased dimerization and activation (Naski et al., 1996). If a similar ligand-independent dimerization explains how the TIE2 mutation causes the vascular changes seen in mucocutaneous VM, it might also explain why these malformations are localized and variable in number, shape, and size. If homodimers of mutant subunits are more active than homo- and heterodimers containing wild-type protein, focal stochastic variations in the expression of the wild-type and mutant alleles could change receptor activity and thus locally modulate TIE2 signaling in ECs. Loss of the wild-type allele (due to a somatic mutation), similar to that recently reported for defects in Gorlin's syndrome (Levanat et al., 1996), may also result in clonal expansion of ECs expressing only the mutant receptor. Such variation in expression could also explain why three family members were carriers of the mutation yet clinically unaffected, reducing the observed penetrance to 94%.

#### The Disproportionate Number of ECs and SMCs in VMs Is Caused by Activation of TIE2

Immunohistochemical analysis showed that the distended vascular channels contain a continuous EC layer surrounded by a highly variable thickness of smooth muscle. Some areas of the channel walls contain a relatively normal number of SMCs, whereas other regions are totally devoid of muscle (Figure 5). The structure of the SMC layer is also disorganized. The diameter of the abnormal vessels can be ten times that of normal channels, suggesting that the dysmorphogenesis involves abnormal venous growth or remodeling caused by a local uncoupling between proliferation and differentiation of ECs and SMCs.

What is already known about the TIE2 signaling pathway supports the hypothesis that it is essential for early vascular development. TIE2 knockout mice and mice with a dominant-negative mutation in TIE2 have 30% and 75% fewer ECs in embryos at days 8.5 and 9.0, respectively, when compared to wild-type embryos (Dumont et al., 1994). The knockout embryos as well as the transgenic embryos die at about embryonic day 9.5–10.5 with malformation of the vascular network (Dumont et al., 1994; Sato et al., 1995), and it has been suggested that TIE2 signaling is important for sprouting and branching or remodeling of the primary capillary plexus (Sato et al., 1995). A gain of function mutation in TIE2

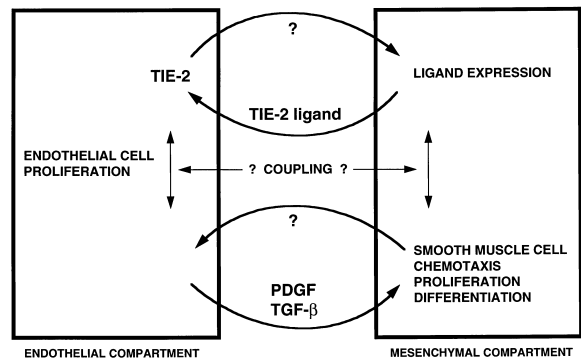


Figure 7. Hypothesis for Coupling of TIE2-Based Signaling in ECs with Recruitment of SMCs in the Vascular Wall

We hypothesize that expression of the TIE2 ligand in mesenchymal cells is controlled by negative feedback from ECs and that this TIE2–ligand loop is coupled to PDGF/TGF $\beta$ -mediated chemotaxis, proliferation, and differentiation of SMCs.

may therefore lead to abnormal sprouting, branching, and remodeling. We believe that the dominantly inherited R849W substitution in the two VM families represents such a gain of function mutation. The lesions contain large venous channels with a disproportionately low number of SMCs. Whether the formation of the abnormal vessels involves abnormal local proliferation of ECs is not known. VM endothelium in a specimen from an 8-year-old girl stained negatively for two proliferating cell markers (Ki-67 and E-selectin) (Kraling et al., 1996), possibly because the VMs examined were established, not growing, lesions.

It is likely that the activity of the TIE2 signaling pathway is at least partially regulated by surrounding mesenchyme since ligands that activate TIE2 are expressed by mesenchymal cells (Davis et al., 1996 [this issue of *Cell*]). Thus, TIE2 signaling in ECs and expression of the ligands in mesenchymal cells are linked. We hypothesize that ligand expression is controlled by a feedback loop, with an EC signal negatively affecting the expression of ligands by SMCs (Figure 7). Furthermore, we suggest that the TIE2 loop is coupled to EC-controlled SMC chemotaxis, proliferation, and differentiation during normal morphogenesis of veins and that it is uncoupled in VMs, since the malformations appear to contain a disproportionate number of ECs relative to investing smooth muscle.

Numerous in vitro and in vivo studies show that PDGF and TGF $\beta$  play major roles in controlling SMC chemotaxis, proliferation, and differentiation. Exogenous PDGF can act as a mitogen and chemoattractant for SMCs and pericytes (Grotendorst et al., 1981; Grotendorst et al., 1982; Westermarck et al., 1990; D'Amore and Smith, 1993). SMCs, reciprocally, can regulate EC expression of PDGF-B, suggesting that there is a feedback loop between the cells in vivo (Bonin and Damon, 1994). Furthermore, the expression patterns of PDGF-B and its receptor PDGF $\beta$ R in angiogenic ECs and surrounding mesenchymal cells as well as data from mice with inactivated PDGF-B and PDGF $\beta$ R alleles suggest that PDGF plays an important role in vascular morphogenesis (Holmgren et al., 1991; Shinbrot et al., 1994;

Soriano, 1994; Leveen et al., 1994). TGF $\beta$ <sub>1</sub> has been shown to be an inhibitor of proliferation of SMCs, though not of pericytes, and a chemoattractant for SMCs (Merwin et al., 1991; D'Amore and Smith, 1993). Also, TGF $\beta$  is activated in EC--SMC cocultures (Antonelli-Orlidge et al., 1989) and TGF $\beta$ <sub>1</sub> is believed to be a regulator of SMC differentiation (Desmouliere et al., 1993). Based on these data, we propose that the TIE2 signaling pathway is coupled to PDGF/TGF $\beta$ -based recruitment of SMCs during vascular morphogenesis (Figure 7). Whether this coupling occurs at the level of endothelial or mesenchymal cells is not clear. If the coupling mechanism is localized in ECs, linking PDGF expression to signaling through TIE2, it would be predicted to be a negative coupling, since the activating TIE2 mutation in VM causes hypoplasia of SMCs and not hyperplasia. This possibility is perhaps less likely, since PDGF expression is usually upregulated in proliferating ECs (Betsholtz, 1993).

The activating mutation in TIE2 is predicted to result in a decreased expression of TIE2 ligands in mesenchymal cells. The more likely possibility is therefore a mechanism that positively couples expression of TIE2 ligands in mesenchymal cells with their PDGF/TGF $\beta$ -mediated migration, proliferation, and differentiation. If this is the case, down-regulation of TIE2 ligand expression (as we predict for VM) should result in decreased SMC recruitment (as we observe in VM), whereas up-regulation of TIE2 ligand expression in mesenchymal cells should result in increased SMC recruitment. Mice carrying conditional knockout alleles or inducible transgenes of TIE2 and TIE2 ligands should be useful in further studies of these possibilities.

## Experimental Procedures

### Family Members

Informed consent was obtained for each family member participating in this study. For family SA (Figure 1A), we collected blood samples from 35 additional family members not previously reported. The Puregene kit was used for DNA extraction following the protocol supplied by the manufacturer (GENTRA Systems). Genotyping of individuals for markers in the 9p region was performed as described earlier (Boon et al., 1994).

### Localization of the TIE2 Gene

To test whether the TIE2 gene is localized in the linked region, we obtained DNA from two human melanoma cell lines known to contain homozygous deletions of the 9p region and from 20 YAC clones located to the same region (kindly provided by Dr. Frank Haluska, Massachusetts Institute of Technology). Cell line W was positive for *IFNA* and *D9S161* but negative for markers *D9S171* and *D9S169*. Cell line MN455 was negative for markers telomeric from *D9S171*, including *IFNA* (F. G. Haluska, unpublished data).

PCR was performed with primers TIE2-3 (sense) 5'-GCAGGAATT GACTGTTCTGC (nt: 3488-3507) and TIE2-4 (antisense) 5'-ATGTCTC CCAAATGTCACCC (nt: 3981-3962), resulting in a 0.9 kb product with genomic DNA as template. PCR reactions were performed in a total volume of 25  $\mu$ l containing 1  $\times$  PCR buffer (Perkin-Elmer), 200  $\mu$ M dNTPs, 0.5  $\mu$ M each primer, and 1 U of Taq polymerase. The 35 cycles consisted of 94°C for 30 s, 54°C for 30 s, and 72°C for 40 s, followed by a final extension step at 72°C for 10 min. To reveal the minimal region where the TIE2 gene can be localized, four additional YAC clones were obtained: 874c7, 822f8, 899b9, and 882f4 (Généthon; clones kindly provided by Dr. J. Vance, Duke University).

### Analysis of the TIE2 Gene

Total RNA was extracted from Epstein-Barr virus-transformed lymphoblasts or peripheral blood leukocytes according to the acid-guanidinium-thiocyanate extraction protocol (Chomczynski and Sacchi, 1987). Five micrograms of total RNA were used as template for cDNA synthesis with oligo(dT) primer using the Superscript Pre-amplification System (GIBCO-BRL).

Nested PCR reactions were performed in a total volume of 50  $\mu$ l under the conditions described above. First-round PCRs were performed for 40 cycles and second-round PCRs for 35 cycles. The cycles consisted of 94°C for 1 min, 56°C or 60°C for 1 min (60°C for 1 min for all second rounds), and 72°C for 2 min (1 min for all second rounds), followed by a final extension step at 72°C for 10 min.

Primers for the first-round PCR reactions were designed so that the 3375 bp coding sequence was amplified in five overlapping fragments. Two nested primer pairs were used for all but the most 3'-end amplification product, yielding nine different second-round fragments. The primers used for PCR and sequencing were as follows (nucleotide positions refer to published cDNA sequence GenBank number L06139, nucleotide number 1 being the adenine in the translation start codon ATG at position 149 in sequence L06139): TIE2-1 (antisense) 5'-TTCTCAGCAGTTGTCAAGGG (nt: 3443-3424); TIE2-2 (sense) 5'-AACCCAGCTGTGCAGTTC AAC (nt: 2372-2391); TIE2-5 (antisense) 5'-TGCCATCCTGGAGAGCAGAG (nt: 1007-988); TIE2-6 (sense) 5'-TGTGAAGCCAGAAAGTGGGG (nt: 631-650); TIE2-7 (sense) 5'-GGACCTCATGCACATTTGTG (nt: -48 to -28); TIE2-8 (antisense) 5'-ACCCATCCTTCTTGATGCGC (nt: 2542-2523); TIE2-9 (sense) 5'-TCTCAAGCACCAGCGGACCT (nt: 2203-2222); TIE2-10 (antisense) 5'-ACTGCAGACCCTTCCAGCCT (nt: 892-873); TIE2-11 (antisense) 5'-CAATGTGCAATACATGTAGGG (nt: 3880-3860); TIE2-12 (sense) 5'-ATTGTCCCGAGGTCAAAGAGG (nt: 2952-2971); TIE2-13 (sense) 5'-GCAAGAATGAAGACCAGCAC (nt: 2033-2052); TIE2-14 (antisense) 5'-ACAAGTCATCCCGCAGTAGG (nt: 3132-3113); TIE2-15 (antisense) 5'-TCCAGCAGAGCCAAGGATGG (nt: 2268-2249); TIE2-16 (antisense) 5'-GAGGGTCACCAGTTCAT GAG (nt: 2196-2177); TIE2-17 (sense) 5'-TATTACCATCCACCGG ATC (nt: 1223-1242); TIE2-18 (sense) 5'-ACTCAGGAGTTTGGGTC TGC (nt: 1253-1272); TIE2-19 (sense) 5'-TCCTGCCTAAAGTCAC ACC (nt: 1652-1671); TIE2-20 (antisense) 5'-AGCACCGAAGTCAAGT TGCC (nt: 1802-1783); TIE2-21 (antisense) 5'-TGATTGGTCCATCCC CAAAG (nt: 1429-1410); TIE2-22 (antisense) 5'-GCTCAGAGCTGATG TTAGTG (nt: 1405-1386); TIE2-23 (sense) 5'-TGCCTCAACAAGCTTC CTTC (nt: 353-372); TIE2-24 (sense) 5'-TATGACTGTGGACAAGG GAG (nt: 390-409); TIE2-25 (sense) 5'-AGAAAGGTGCAGTGGAC AAG (nt: 795-814); TIE2-26 (antisense) 5'-GCATGAGGCAGGTGTAC TTC (nt: 542-523); TIE2-27 (sense) 5'-TGGAAAGTCACAAACCGCTG (nt: -88 to -69); TIE2-28 (antisense) 5'-GGGCACTGAATGATGA AGG (nt: 498-479); TIE2-29 (sense) 5'-TTCAGTATCAGCTCAAGGGC (nt: 2084-2103); TIE2-30 (antisense) 5'-GTGTGCCTCCTAAGCTA ACA (nt: 3112-3093); and TIE2-31 (antisense) 5'-TCATTCCTTTGATG GCAGCATC (nt: 2572-2551).

The five primer pairs used for the first-round PCRs were TIE2-11/TIE2-12, TIE2-13/TIE2-14, TIE2-15/TIE2-17, TIE2-21/TIE2-23, and TIE2-26/TIE2-27. The nested primer pairs used for the second-round PCR for each of these first-round PCRs were, respectively, TIE2-3/TIE2-4, TIE2-1/TIE2-12, TIE2-2/TIE2-30, TIE2-8/TIE2-29, TIE2-16/TIE2-19, TIE2-18/TIE2-20, TIE2-10/TIE2-24, TIE2-22/TIE2-25, and TIE2-7/TIE2-28.

To sequence the mutation site from genomic DNA, primers TIE2-2570 (sense) 5'-TCAGGGACTCTGGCCCTAAACAG (nt: 2392-2414) and TIE2-577-ER (antisense) 5'-ATATTCCTTTCATTCTTTGATG GCAGCATC (nt: 2580-2551) were used. Allele-specific PCR was used to screen family members and controls. Two additional primers with similar estimated annealing temperatures were synthesized: TIE2-R (antisense) 5'-TTGATGGCAGCATCCATCCG (nt: 2564-2545), TIE2-W (antisense) 5'-TTTGATGGCAGCATCCATCCA (nt: 2565-2545). The analyses were performed using two separate PCRs for each template: TIE2-2/TIE2-R or TIE2-2/TIE2-W, both containing an internal control, TIE2-6/TIE2-10 (Figure 2B). The reaction conditions were the same as mentioned above, except that the nucleotide concentration was 40  $\mu$ M. Each cycle of the PCR consisted of 95°C for 1 min, 68°C for 1 min, and 72°C for 1 min (30 cycles), with a final extension at 72°C for 10 min. Cosegregation of the mutation in family

AF was studied using MaeIII restriction enzyme digestions of TIE2-2570/TIE2-577-ER amplification products. This 189 bp PCR product contains one MaeIII site (at nt 149) that is abolished by the mutation.

#### Construction of Full-Length Clones of the TIE2 Gene and Their Expression Using a Baculovirus Expression System

To clone the 3375 bp coding sequence of the TIE2 gene, cDNA synthesized as described above was used as template for nested PCR. First-round PCR using primers TIE2-4/TIE2-27 and second-round PCR with primers TIE2-1/TIE2-7 were performed under conditions as described above, except that Taq extender was used according to the manufacturer's directions (Stratagene). Each cycle consisted of 94°C for 1 min, 60°C for 1 min, and 72°C for 5 min, with a final extension at 72°C for 10 min, for a total of 40 cycles for the first round, and 94°C for 1 min, 60°C for 1 min, and 72°C for 4 min, with a final extension at 72°C for 10 min, for a total of 35 cycles for the second round. This full-length amplification product was purified using Centricon-100 columns (Amicon) and cloned into the pGemT-vector (Promega). A clone (#1/#4) containing the full-length TIE2 coding sequence was cycle-sequenced (Perkin-Elmer). Taq-polymerase errors were eliminated from the clone by exchanging regions between unique restriction enzyme cutting sites in the construct, with corresponding fragments amplified from lymphoblast-derived cDNA with Pfu DNA polymerase (Stratagene). Similarly, the mutation site in the original clone was replaced by the corresponding wild-type sequence. The full-length inserts were cloned into the baculovirus expression vector BacPAK8 (Clontech), and the full-length clones, BP-TIE2-R2 and BP-TIE2-W2, were checked by sequencing. Neither of the clones contained the variant valine 788. No nucleotide changes resulting in amino acid changes were present, other than the introduced C-to-T substitution in the BP-TIE2-W2 clone.

Recombinant baculoviruses encoding wild-type and mutated TIE2 were produced in Sf9 insect cells with the BP-TIE2-R2 and BP-TIE2-W2 constructs using the Linear AcNPV Transfection Kit (Invitrogen), according to the manufacturer's directions. Recombinant viruses were plaque-purified prior to use. For kinase assays,  $5 \times 10^7$  Sf9 cells were infected with wild-type, TIE2-R2, or TIE2-W2 baculovirus at a multiplicity of infection of 10–30. Seventy-two hours after infection, cells were harvested and membranes were prepared as previously described (Guy et al., 1992). Membranes were solubilized in lysis buffer (20 mM HEPES/Na [pH 7.4], 150 mM NaCl, 1 mM EDTA, 1% NP-40, 1 mM orthovanadate, 1 mM PMSF, and 1  $\mu$ g/ml each of leupeptin, aprotinin, and pepstatin A), and particulate matter was cleared by centrifugation at  $12,000 \times g$  for 15 minutes. The supernatants were immunoprecipitated with 1  $\mu$ g anti-TIE2 antibody C-20 (Santa Cruz) and 30  $\mu$ l Protein A Sepharose, and precipitates were used to phosphorylate an oriented random peptide library with [ $\gamma$ -<sup>32</sup>P]ATP. Library phosphorylations were carried out as described previously (Songyang et al., 1995), except that 0.05% Triton X-100 was added to the kinase reaction buffer. The radioactivity associated with the peptide library was determined after 2 hr of phosphorylation, and the immunoprecipitates were analyzed by 6% SDS polyacrylamide gel electrophoresis followed by immunoblotting with 0.2  $\mu$ g/ml anti-TIE2 C-20 and visualization by enhanced chemiluminescence. In some experiments, infected insect cells were solubilized directly in lysis buffer, and the tyrosine phosphorylation state of TIE2 receptors was assessed by immunoblotting with anti-phosphotyrosine antibody RC20 (Transduction Laboratories) followed by enhanced chemiluminescence.

#### Immunohistochemistry

Paraffin blocks of surgically resected VMs were collected for individuals II-5, II-7, II-8, II-14, and III-7. Sections of 6–8  $\mu$ m were cut and attached to Superfrost Plus slides (Fisher Scientific). Deparaffinization by histosol was followed by rehydration through a gradient of ethanol and distilled water.

Hematoxylineosin staining was performed using Harris Modified Hematoxylin (Fisher Scientific) and Alcoholic Eosin Yellowish Solution (Fisher Scientific). The antibodies used for this study, antihuman CD31 murine monoclonal antibody (Dako), antihuman vWF murine monoclonal antibody (Dako), antihuman  $\alpha$ -SMC actin murine monoclonal antibody (Dako), and alkaline phosphatase-conjugated goat

antimouse antibody (Promega), were kindly provided by Dr. K. Takahashi (Takahashi et al., 1994).

Prior to staining for antibodies, the tissues were incubated with 250  $\mu$ g/ml protease (Sigma Chemical) for 6 mins. Blocking was performed by incubating the slides in 5% skim milk with PBS for 1 hr. Primary antibodies (diluted 1:100 in PBS) were applied at 4°C for 12 hr. After washing with PBS, the secondary antibody (diluted 1:100 in PBS) was applied for 1 hr at room temperature. Fast-red chromogen (Dako) was used for visualization of the immunoreactions. The reactions were terminated by adding water, and the slides were mounted using Permount (Fisher Scientific).

#### Acknowledgments

The project was supported by the Finnish Cultural Foundation, the Academy of Finland (M. V.), Catholic University of Louvain, Belgium, The Foundation for Faces of Children (L. M. B.), American Heart Association–Sanofi-Winthrop award 95006970, the Baxter Foundation, Sandoz Pharmaceuticals (D. A. M.), the M. B. Gold Family (M. L. W.), the Lucille P. Markey Charitable Trust (L. C. C.), Organogenesis Inc., and National Institutes of Health grant HL33014 (B. R. O.). M. V. is recipient of a Fogarty International Research Fellowship Award; J. T. C. is recipient of a National Science Foundation predoctoral fellowship; and D. A. M. is an Established Investigator of the American Heart Association. We are grateful to all patients and family members who participated in the study. We also thank Dr. K. Alitalo for the TIE2 clone, Dr. F. Haluska for YAC clones and melanoma cell lines, and Dr. J. Vance for YAC clones. Y. Pittel provided expert secretarial assistance.

Received October 28, 1996; revised November 21, 1996.

#### References

- Allen, K.E., Varty, K., Jones, L., Sayers, R.D., Bell, P.R., and London, N.J. (1994). Human venous endothelium can promote intimal hyperplasia in a paracrine manner. *J. Vasc. Surg.* 19, 577–584.
- Antonelli-Orlidge, A., Saunders, K.B., Smith, S.R., and D'Amore, P.A. (1989). An activated form of transforming growth factor beta is produced by cocultures of endothelial cells and pericytes. *Proc. Natl. Acad. Sci. USA* 86, 4544–4548.
- Bellus, G.A., Hefferon, T.W., Ortiz de Luna, R.I., Hecht, J.T., Horton, W.A., Machado, M., Kaitila, I., McIntosh, I., and Francomano, C.A. (1995). Achondroplasia is defined by recurrent G380R mutations of FGFR3. *Am. J. Hum. Genet.* 56, 368–373.
- Betsholtz, C. (1993). The PDGF genes and their regulation. In *Biology of Platelet-Derived Growth Factor*. Cytokines, B. Westermarck and C. Sorg, eds. (Basel: Karger), pp. 11–30.
- Bonin, L.R., and Damon, D.H. (1994). Vascular cell interactions modulate the expression of endothelin-1 and platelet-derived growth factor BB. *Am. J. Physiol.* 267, H1698–H1706.
- Boon, L.M., Mulliken, J.B., Vikkula, M., Watkins, H., Seidman, J., Olsen, B.R., and Warman, M.L. (1994). Assignment of a locus for dominantly inherited venous malformations to chromosome 9p. *Hum. Mol. Genet.* 3, 1583–1587.
- Chomczynski, P., and Sacchi, N. (1987). Single-step method of RNA isolation by acid guanidinium thiocyanate-phenol-chloroform extraction. *Anal. Biochem.* 162, 156–159.
- D'Amore, P.A., and Smith, S.R. (1993). Growth factor effects on cells of the vascular wall: a survey. *Growth Factors* 8, 61–75.
- Davis, S., Aldrich, T.H., Jones, P.F., Acheson, A., Compton, D.L., Jain, V., Ryan, T.E., Bruno, J., Radziejewski, C., Maisonpierre, P.C., et al. (1996). Isolation of Angiopoietin-1, a ligand for the TIE2 receptor, by secretion-trap expression cloning. *Cell* 87, this issue.
- Desmouliere, A., Geinoz, A., Gabbiani, F., and Gabbiani, G. (1993). Transforming growth factor-beta 1 induces alpha-smooth muscle actin expression in granulation tissue myofibroblasts and in quiescent and growing cultured fibroblasts. *J. Cell Biol.* 122, 103–111.
- Dumont, D.J., Anderson, L., Breitman, M.L., and Duncan, A.M.

- (1994). Assignment of the endothelial-specific protein receptor tyrosine kinase gene (TEK) to human chromosome 9p21. *Genomics* 23, 512–513.
- Dumont, D.J., Gradwohl, G., Fong, G.H., Puri, M.C., Gertsenstein, M., Auerbach, A., and Breitman, M.L. (1994). Dominant-negative and targeted null mutations in the endothelial receptor tyrosine kinase, tek, reveal a critical role in vasculogenesis of the embryo. *Genes Dev.* 8, 1897–1909.
- Dumont, D.J., Fong, G.H., Puri, M.C., Gradwohl, G., Alitalo, K., and Breitman, M.L. (1995). Vascularization of the mouse embryo: a study of flk-1, tek, tie, and vascular endothelial growth factor expression during development. *Dev. Dyn.* 203, 80–92.
- Fillinger, M.F., O'Connor, S.E., Wagner, R.J., and Cronenwett, J.L. (1993). The effect of endothelial cell coculture on smooth muscle cell proliferation. *J. Vasc. Surg.* 17, 1058–1067.
- Gallione, C.J., Pasyk, K.A., Boon, L.M., Lennon, F., Johnson, D.W., Helmbold, E.A., Markel, D.S., Vikkula, M., Mulliken, J.B., Warman, M.L., et al. (1995). A gene for familial venous malformations maps to chromosome 9p in a second large kindred. *J. Med. Genet.* 32, 197–199.
- Grotendorst, G.R., Seppa, H.E., Kleinman, H.K., and Martin, G.R. (1981). Attachment of smooth muscle cells to collagen and their migration toward platelet-derived growth factor. *Proc. Natl. Acad. Sci. USA* 78, 3669–3672.
- Grotendorst, G.R., Chang, T., Seppa, H.E., Kleinman, H.K., and Martin, G.R. (1982). Platelet-derived growth factor is a chemoattractant for vascular smooth muscle cells. *J. Cell. Physiol.* 113, 261–266.
- Guy, P.M., Carraway, K.L. III, and Cerione, R.A. (1992). Biochemical comparisons of the normal and oncogenic forms of insect cell-expressed neu tyrosine kinases. *J. Biol. Chem.* 267, 13851–13856.
- Holmgren, L., Glaser, A., Pfeifer-Ohlsson, S., and Ohlsson, R. (1991). Angiogenesis during human extraembryonic development involves the spatiotemporal control of PDGF ligand and receptor gene expression. *Development* 113, 749–754.
- Johnson, D.W., Berg, J.N., Baldwin, M.A., Gallione, C.J., Marondel, I., Yoon, S.J., Stenzel, T.T., Speer, M., Pericak-Vance, M.A., Diamond, A., et al. (1996). Mutations in the activin receptor-like kinase 1 gene in hereditary haemorrhagic telangiectasia type 2. *Nature Genet.* 13, 189–195.
- Kaipainen, A., Korhonen, J., Mustonen, T., van Hinsbergh, V.W., Fang, G.H., Dumont, D., Breitman, M., and Alitalo, K. (1995). Expression of the fms-like tyrosine kinase 4 gene becomes restricted to lymphatic endothelium during development. *Proc. Natl. Acad. Sci. USA* 92, 3566–3570.
- Kirby, M.L., and Waldo, K.L. (1995). Neural crest and cardiovascular patterning. *Circ. Res.* 77, 211–215.
- Kraling, B.M., Razon, M.J., Boon, L.M., Zurakowski, D., Seachord, C., Darveau, R.P., Mulliken, J.B., Corless, C.L., and Bischoff, J. (1996). E-selectin is present in proliferating endothelial cells in human hemangiomas. *Am. J. Pathol.* 148, 1181–1191.
- Levanat, S., Gorlin, R.J., Fallet, S., Johnson, D.R., Fantasia J.E., and Bale, A.E. (1996). A two-hit model for developmental defects in Gorlin syndrome. *Nature Genet.* 12, 85–87.
- Leveen, P., Pekny, M., Gebre-Medhin, S., Swolin, B., Larsson, E., and Betsholtz, C. (1994). Mice deficient for PDGF B show renal, cardiovascular, and hematological abnormalities. *Genes Dev.* 8, 1875–1887.
- McAllister, K.A., Grogg, K.M., Johnson, D.W., Gallione, C.J., Baldwin, M.A., Jackson, C.E., Helmbold, E.A., Markel, D.S., McKinnon, W.C., Murrell, J., et al. (1994). Endoglin, a TGF-beta binding protein of endothelial cells, is the gene for hereditary haemorrhagic telangiectasia type 1. *Nature Genet.* 8, 345–351.
- Merwin, J.R., Newman, W., Beall, L.D., Tucker, A., and Madri, J. (1991). Vascular cells respond differentially to transforming growth factors beta 1 and beta 2 in vitro. *Am. J. Pathol.* 138, 37–51.
- Mohammadi, M., Schlessinger, J., and Hubbard, S.R. (1996). Structure of the FGF receptor tyrosine kinase domain reveals a novel autoinhibitory mechanism. *Cell* 86, 577–587.
- Mulliken, J.B., and Young, A.E. (1988). Vascular birthmarks. In *Hemangiomas and Malformations*, J.B. Mulliken and A.E. Young, eds. (Philadelphia: W.B. Saunders).
- Nakamura, H. (1988). Electron microscopic study of the prenatal development of the thoracic aorta in the rat. *Am. J. Anat.* 181, 406–418.
- Naski, M.C., Wang, Q., Xu, J., and Ornitz, D.M. (1996). Graded activation of fibroblast growth factor receptor 3 by mutations causing achondroplasia and thanatophoric dysplasia. *Nature Genet.* 13, 233–237.
- Noden, D.M. (1989). Embryonic origins and assembly of blood vessels. *Am. Rev. Respir. Dis.* 140, 1097–1103.
- Orlidge, A., and D'Amore, P.A. (1987). Inhibition of capillary endothelial cell growth by pericytes and smooth muscle cells. *J. Cell Biol.* 105, 1455–1462.
- Powell, R.J., Carruth, J.A., Basson, M.D., Bloodgood, R., and Sumpio, B.E. (1996a). Matrix-specific effect of endothelial control of smooth muscle cell migration. *J. Vasc. Surg.* 24, 51–57.
- Powell, R.J., Cronenwett, J.L., Fillinger, M.F., Wagner, R.J., and Sampson, L.N. (1996b). Endothelial cell modulation of smooth muscle cell morphology and organizational growth pattern. *Ann. Vasc. Surg.* 10, 4–10.
- Risau, W., and Lemmon, V. (1988). Changes in the vascular extracellular matrix during embryonic vasculogenesis and angiogenesis. *Dev. Biol.* 125, 441–450.
- Risau, W., Sariola, H., Zerwes, H.G., Sasse, J., Ekblom, P., Kemler, R., and Doetschman, T. (1988). Vasculogenesis and angiogenesis in embryonic-stem-cell-derived embryoid bodies. *Development* 102, 471–478.
- Sato, T.N., Tozawa, Y., Deutsch, U., Wolburg-Buchholz, K., Fujiwara, Y., Gendron-Maguire, M., Gridley, T., Wolburg, H., Risau, W., and Qin, Y. (1995). Distinct roles of the receptor tyrosine kinases Tie-1 and Tie-2 in blood vessel formation. *Nature* 376, 70–74.
- Savitsky, K., Bar-Shira, A., Gilad, S., Rotman, G., Ziv, Y., Vanagaite, L., Tagle, D.A., Smith, S., Uziel, T., Sfez, S., et al. (1995). A single ataxia telangiectasia gene with a product similar to PI-3 kinase. *Science* 268, 1749–1753.
- Shah, N.M., Groves, A.K., and Anderson, D.J. (1996). Alternative neural crest cell fates are instructively promoted by TGFβ superfamily members. *Cell* 85, 331–343.
- Shinbrot, E., Peters, K.G., and Williams, L.T. (1994). Expression of the platelet-derived growth factor beta receptor during organogenesis and tissue differentiation in the mouse embryo. *Dev. Dyn.* 199, 169–175.
- Songyang, Z., Carraway, K.L., Eck, M.J., Harrison, S.C., Feldman, R.A., Mohammadi, M., Schlessinger, J., Hubbard, S.R., Smith, D.P., Eng, C., et al. (1995). Catalytic specificity of protein-tyrosine kinases is critical for selective signaling. *Nature* 373, 536–539.
- Soriano, P. (1994). Abnormal kidney development and hematological disorders in PDGF beta-receptor mutant mice. *Genes Dev.* 8, 1888–1896.
- Takahashi, K., Mulliken, J.B., Kozakewich, H.P., Rogers, R.A., Folkman, J., and Ezekowitz, R.A. (1994). Cellular markers that distinguish the phases of hemangioma during infancy and childhood. *J. Clin. Invest.* 93, 2357–2364.
- Webster, M.K., d'Avis, P.Y., Robertson, S.C., and Donoghue, D.J. (1996). Profound ligand-independent kinase activation of fibroblast growth factor receptor 3 by the activation loop mutation responsible for a lethal skeletal dysplasia, thanatophoric dysplasia type II. *Mol. Cell. Biol.* 16, 4081–4087.
- Westermark, B., Siegbahn, A., Heldin, C.H., and Claesson-Welsh, L. (1990). B-type receptor for platelet-derived growth factor mediates a chemotactic response by means of ligand-induced activation of the receptor protein-tyrosine kinase. *Proc. Natl. Acad. Sci. USA* 87, 128–132.